Artificial Metalloenzymes

International Edition: DOI: 10.1002/anie.201508816
German Edition: DOI: 10.1002/ange.201508816

Genetic Optimization of Metalloenzymes: Enhancing Enzymes for Non-Natural Reactions

Todd K. Hyster and Thomas R. Ward**

Keywords:
asymmetric synthesis · directed evolution · hybrid catalysts · metalloenzymes

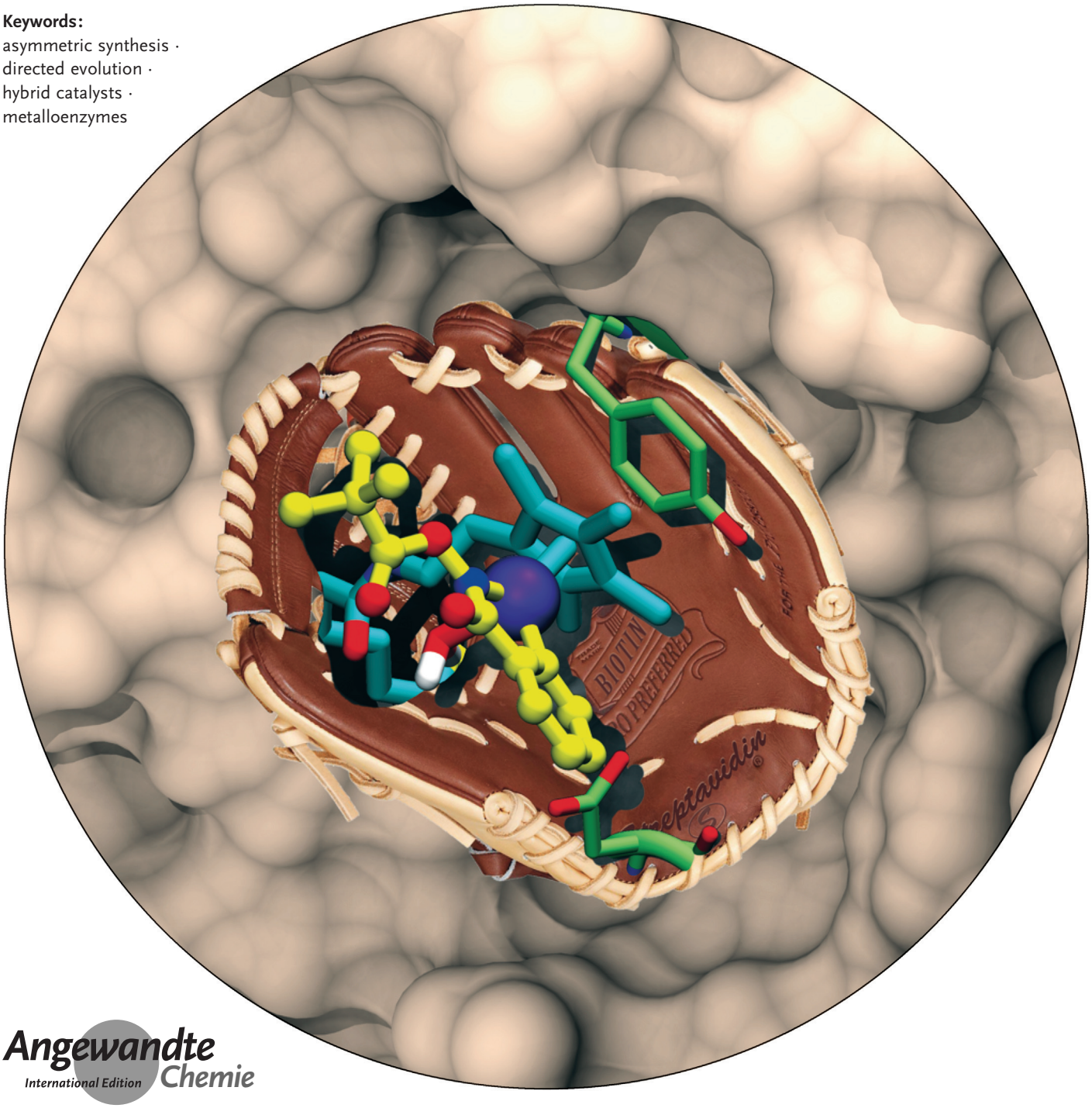

Artificial metalloenzymes have received increasing attention over the last decade as a possible solution to unaddressed challenges in synthetic organic chemistry. Whereas traditional transition-metal catalysts typically only take advantage of the first coordination sphere to control reactivity and selectivity, artificial metalloenzymes can modulate both the first and second coordination spheres. This difference can manifest itself in reactivity profiles that can be truly unique to artificial metalloenzymes. This Review summarizes attempts to modulate the second coordination sphere of artificial metalloenzymes by using genetic modifications of the protein sequence. In doing so, successful attempts and creative solutions to address the challenges encountered are highlighted.

From the Contents

1. Introduction 7345
2. Natural Metalloenzymes that Catalyze Non-Natural Reactions 7346
3. Supramolecular Docking 7349
4. Covalent Anchoring 7354
5. Artificial Hydrolases 7354
6. Outlook 7356

1. Introduction

Biocatalysis has evolved from a field of research that observes the natural catalytic properties of enzymes to one that expands the reactivity of existing enzymes and creates entirely new enzymes with reactivity never before seen in nature.[1] This development was largely spurred by advances in molecular biology and the development of systematic methods for altering protein properties through iterative rounds of genetic modification (i.e. directed evolution).[2,3] Directed evolution efforts have primarily targeted broadening solvent tolerance, increasing temperature stability, expanding substrate scope, and increasing reaction selectivity (enantio-, diastereo-, regio-, and chemoselectivity).[3] The catalysts accessed through directed evolution are superb catalytic species, capable of providing synthetic methods with superior efficiency to those achieved using small-molecule catalysts.[4] The chief limitation to further adoption of biocatalytic processes is the breadth of reactions accessible to this catalytic manifold.

Addressing this limited reaction scope has become the focus of intense interest in the last decade.[5] The pursuit of catalytic promiscuity in biocatalysis has largely centered on finding new reactions that proceed by mechanisms that rely on intermediates that are similar to those of the natural reaction. This is perhaps best epitomized in the lipase literature, where common hydrolases are shown to be effective catalysts for Aldol, Michael, and Mannich reactions, among many others.[6] After the discovery of new reactivity, the promiscuous function can be further optimized by extensive protein engineering.[2d,7] Although effective, this approach is restricted to reactions that share mechanistic similarities with natural reactions. As a consequence, large swaths of non-natural reactions are inaccessible by this method. In particular, the wealth of reactions catalyzed by transition metals are largely inaccessible. An approach to encompass these reactions is to place a transition metal into the active site of a protein, either in the form of artificial metalloenzymes or natural metalloenzymes, and explore their potential to catalyze reactions that the metal cofactor may catalyze independently.

An early manifestation of this goal was the formation of artificial metalloenzymes, where a catalytically active transition metal is selectively incorporated into a protein scaffold. In the mid-1970s the Kaiser and Whitesides research groups demonstrated that such hybrid catalysts could be formed and provide catalytic activity for oxidation and reduction reactions.[8,9] Since these seminal reports, studies in the field have largely focused on how to selectively introduce different transition-metal complexes into a variety of protein scaffolds through dative, covalent, or supramolecular anchoring while maintaining or enhancing the catalytic activity of the metal.[10] A complementary approach is to use proteins that have a natural affinity for a cofactor capable of catalyzing non-natural reactions in the absence of the protein scaffold. Both of these approaches represent only the first step in developing metalloenzyme catalysts capable of effecting non-natural reactions. To create a hybrid that truly benefits from both the protein and transition-metal components, the protein component must be genetically engineered for the desired traits. Although genetic modification of natural enzymes is routinely applied in both academia and industry, the same does not hold true for artificial metalloenzymes.[11] Perhaps the greatest challenge towards the directed evolution of artificial metalloenzymes is to maintain the catalytic efficiency of the cofactor in the presence of unpurified protein samples.[12] Indeed, many organometallic cofactors are inhibited in the presence of cellular extracts (e.g. DNA, proteins, metabolites, lipids etc.). This sets a stringent requirement on the use of purified protein samples for the optimization of artificial metalloenzymes. This prerequisite thus limits the number of samples that can be screened, as parallel protein purification is time consuming.

[*] Prof. T. K. Hyster
Department of Chemistry, Princeton University
Princeton, NJ 08544 (USA)
E-mail: thyster@princeton.edu
Prof. T. R. Ward
Department of Chemistry, University of Basel
Spitalstrasse 51, CH-4056 Basel (Switzerland)
E-mail: thomas.ward@unibas.ch

This Review summarizes the efforts towards the genetic optimization of artificial metalloenzymes in terms of catalytic reactivity and selectivity. Genetic modifications of protein scaffolds to enable docking of a transition metal (i.e. bioconjugation) have recently been reviewed and will not be further discussed herein.[10] Our aim is to identify broadly applicable strategies for genetically engineering metalloenzymes. Ultimately, these should be relevant toward other types of metalloenzymes and thus expand the field from one that looks simply to find effective hybrid catalysts to one that aims at exploiting these systems to address challenges that neither small molecules catalysts nor enzymes can currently address. Two complementary strategies are summarized in this review: 1) repurposing natural metalloenzymes towards non-natural reactions (Sections 2 and 6) and 2) introducing an abiotic cofactor within a protein scaffold to generate artificial metalloenzymes (Sections 3–5). Artificial metalloenzymes resulting from chemically synthesized host protein/peptides (i.e. solid-phase synthesis) have been recently reviewed and will not be presented herein.[10] The focus of this Review is set on the genetic strategies for the optimization of the performance of (artificial) metalloenzymes.

2. Natural Metalloenzymes that Catalyze Non-Natural Reactions

2.1. Cytochrome P450s

Cytochrome P450s are widespread and powerful enzymes that oxidize olefins, heteroatoms, and inert C–H bonds by using molecular oxygen or hydrogen peroxide as the oxidant.[13] Essential for this reactivity is the iron porphyrin heme cofactor. Aside from effecting oxygenation, iron porphyrins are known to catalyze the cyclopropanation of alkenes with diazoesters.[14] Arnold was interested in exploring the ability of cytochrome P450s to catalyze carbene transfer reactions.[15] In a seminal report, $P450_{BM3}$ was shown to be an effective catalyst for the cyclopropanation of styrenes when using ethyl diazoacetate (EDA) as a carbene source under anaerobic conditions, thereby providing product with low conversion and selectivity (TTN 5; TTN = total turnover number).[16] A single mutation of the conserved distal threonine (T268), hypothesized to facilitate proton transfer in the natural reactivity, to alanine ($P450_{BM3}$-T268A) enabled *trans*-selective cyclopropanation in high yield and enantioselectivity

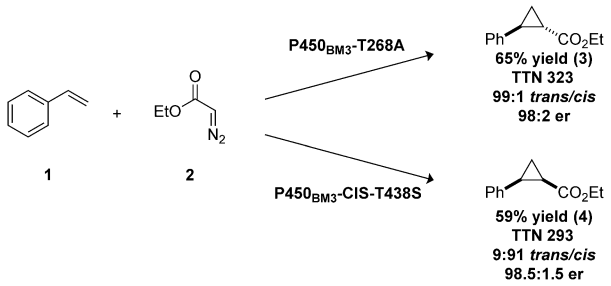

Figure 1. Repurposing cytochrome P450 as an artificial cyclopropanase under anaerobic conditions. The catalytic performance is improved by genetic modification of the second coordination sphere of the heme cofactor. Whereas *trans* selectivity requires a single point mutation (top), the *cis*-cyclopropanase bears 15 mutations compared to WT $P450_{BM3}$ (bottom). $P450_{BM3}$-CIS-T438S = V78A, F87V, P142S, T175I, A184V, S226R, H236Q, E252G, T268A, A290V, L353V, I366V, T438S, E442K.

(Figure 1, top). The *cis* diastereomer was accessed preferentially in modest yield and diastereoselectivity but with excellent enantioselectivity by using a variant that contained 14 mutations from the wild-type enzyme ($P450_{BM3}$-CIS). The introduction of serine at position T438 ($P450_{BM3}$-CIS-T438S), improved the diastereoselectivity to $>9{:}1$ as well as the enantioselectivity and the yield (Figure 1, bottom). A small library of structurally distinct $P450_{BM3}$ mutants allowed the selective cyclopropanation of a diverse set of styrenes. This library was also effective for the insertion of carbenes into N–H bonds.[17] Preliminary mechanistic studies suggest that Fe^{II} is the resting state of the heme cofactor. This feature presents a challenge when attempting to reduce heme from Fe^{III} to Fe^{II} under physiological conditions, as cytochrome P450 enzymes have an elaborate gating mechanism to prevent electron transfer in the absence of substrate. Given the low affinity of the substrates for the protein's active site, the desired conformational change is not possible.

To facilitate reduction, Arnold and co-workers explored the impact of heme ligation on the redox potential of the heme cofactor.[18] Remarkably, mutating the cysteine to the isosteric serine shifts the redox potential from −430 mV ($E^{0\prime}\,Fe^{III}/Fe^{II}_{cys}$) to −293 mV ($E^{0\prime}\,Fe^{III}/Fe^{II}_{ser}$). The resulting $P450_{BM3}$-C400S variant, referred to as $P411_{BM3}$ (named for the shift in the diagnostic CO Soret band), possesses a redox potential well within the range for the biological reductant NADPH ($E^{0\prime}_1 = -320$ mV). Furthermore, $P411_{BM3}$ has poor

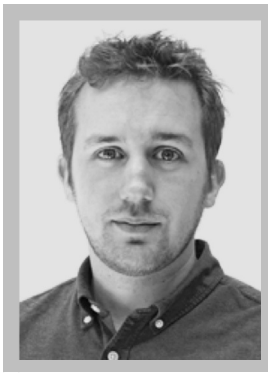

Todd K Hyster received his BS from the University of Minnesota in 2008. He performed his graduate studies at Colorado State University under the guidance of Prof. Tomislav Rovis. During his studies, he spent time as a Marie Curie fellow in the group of Prof. Thomas R. Ward at the University of Basel. After obtaining his PhD in 2013, he joined the group of Prof. Frances H. Arnold at the California Institute of Technology, as an NIH postdoctoral fellow. In 2015, he began his independent career at Princeton University.

Thomas R. Ward received his PhD from ETH Zürich (with L. M. Venanzi, 1991). After two postdoctorial positions (with R. Hoffmann, Cornell Univ., and C. Floriani, Univ. Lausanne), he started his independent career at the University of Berne in 1993 as a Werner fellow. He was full professor at the University of Neuchâtel (2000–2008) before joining the University of Basel. His research interests are centered primarily on the creation and optimization of artificial metalloenzymes by anchoring abiotic cofactors within host proteins.

oxygenase reactivity, thus eliminating undesired formation of styrene oxide. Finally, the efficiency with which the $P411_{BM3}$ effects the desired transformation is roughly four times greater that of $P450_{BM3}$ (Figure 2, top). At high substrate concentrations, the best catalyst ($P411_{BM3}$-CIS-T438S) effected the *cis*-selective cyclopropanation with a TTN of >67000 and a selectivity that was nearly identical to that achieved by the $P450_{BM3}$-CIS-T438S variant (90:10 d.r., 99% *ee*). Crystallographic data suggests that mutation of the axial cysteine to serine does not have a significant impact on the overall fold of the protein (0.52 Å r.m.s. deviation from $P450_{BM3}$; r.m.s. = root mean square). The introduction of the key axial serine mutation into other P450 scaffolds yields catalysts that are more effective for cyclopropanation than the parent metalloenzyme.[19]

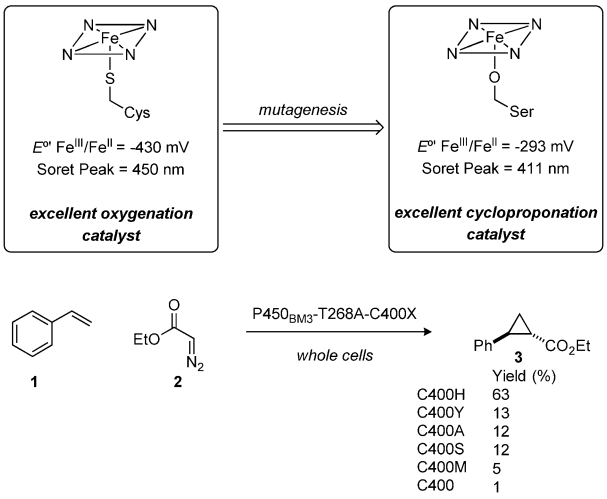

Figure 2. Top: Mutation of the axial cysteine C400 to serine significantly affects the reduction potential of the heme moiety and shifts the Soret band from 450 nm to 411 nm. The repurposed cytochrome P411 completely loses its monooxygenase activity in favor of cyclopropanation activity. Bottom: Activity of various axial ligands for styrene cyclopropanation.

The axial mutation was further expanded to include residues that are not isosteric with cysteine.[20,21] This modest screening effort led to the identification of histidine (i.e. T268A-C400H) as the most efficient artificial metalloenzyme for the cycloproponation of styrene with EDA (Figure 2, bottom).[70] This engineered variant was applied to the formal synthesis of levomilnacipran, where T268A-C400H provided the precursor cyclopropane in excellent yield and diastereoselectivity, but modest enantioselectivity. After three rounds of site-saturation mutagenesis targeting residues located within the protein's active site, a variant (T268A-C400H-T438W-V78M-L181V, coined Hstar) was identified that provided the cyclopropane precursor to levomilnacipran in high yield and excellent enantioselectivity, even under aerobic conditions (Figure 3). Gratifyingly and in contrast to many biocatalysts, Hstar is a fairly general catalyst that furnishes high yields and selectivity for an array of substituted acrylamides.[22]

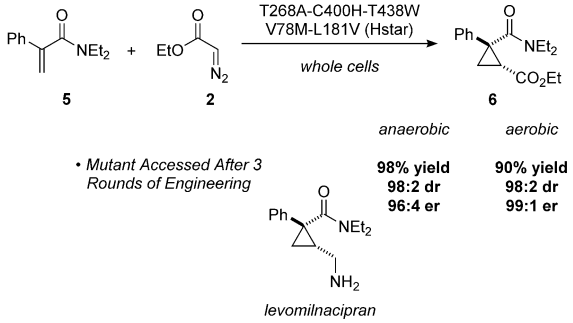

Figure 3. Directed evolution of the artificial cyclopropanase Hstar for the synthesis of a levomilnacipran precursor.

The P411 scaffold is also effective for nitrene transfer reactions. Arnold and co-workers found that $P411_{BM3}$-T268A could effect benzylic C–H amination on 1,3,5-triethylbenzenesulfonylazide (**7**), albeit in modest yield.[23] In contrast to the carbene transfer reactivity, Arnold and co-workers found that $P450_{BM3}$-based catalysts were inefficient for this type of reactivity. Engineering the protein scaffold to a variant bearing an additional 15 mutations from WT-$P450_{BM3}$ ($P411_{BM3}$-CIS-T438S) improved the yield to nearly 70% (430 TTN) and excellent enantioselectivity (87% *ee*; Figure 4) in whole cells. The impact of the active site

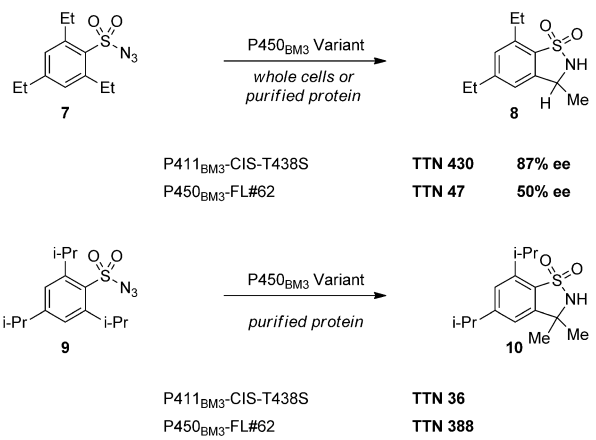

Figure 4. Nitrene insertion catalyzed by cytochrome $P411_{BM3}$ and $P450_{BM3}$. $P411_{BM3}$-CIS-T438S = V78A, F87V, P142S, T175I, A184V, S226R, H236Q, E252G, T268A, A290V, L353V, I366V, C400S, T438S, E442K. $P450_{BM3}$-#FL62 = V87A, F81S, A82V, F87A, P142S, T175I, A180T, A184V, A197V, F205C, S226R, H236Q, E252G, R255S, A290V, L353V.

architecture is critically important when considering nitrene transfer reactions in the active site of the protein. Arnold and co-workers found that triethylbenzenesulfonylazide (**7**) is more effective than triisopropylbenzenesulfonylazide (**9**), despite the lower bond dissociation energy of the later substrate (85 compared to 83 kcal mol^{-1}). Fasan and co-workers observed the opposite trend in subsequent work using other P450 variants ($P450_{BM3}$-FL#62), where **9** was more effective than **7** (Figure 4).[24] Possible explanations for this difference include the differing heme ligation in the two

studies or the differing active-site architectures of the variants used in each study.

The initial reports on P450-catalyzed C–H amination exclusively reported amination of the weakest C–H bond present in the substrate. Arnold and co-workers found that the strong C–H bonds could be selectively aminated in the presence of weak C–H bonds through systematic modulation of the active-site architecture.[25] Amination of the strong homobenzylic C–H bonds can be achieved with dipropyl benzenesulfonylazide **11** when a P411 variant containing phenylalanine at position I263F is used (97:3 selectivity over benzylic amination; Figure 5). The selectivity can be reversed in favor of the benzylic amination on the same substrate using P411BM3-F87A-T268A). Such a remarkable regiodivergency is difficult to achieve with small-molecule catalysts and highlights the potential of biocatalytic solutions to complement small-molecule methods.

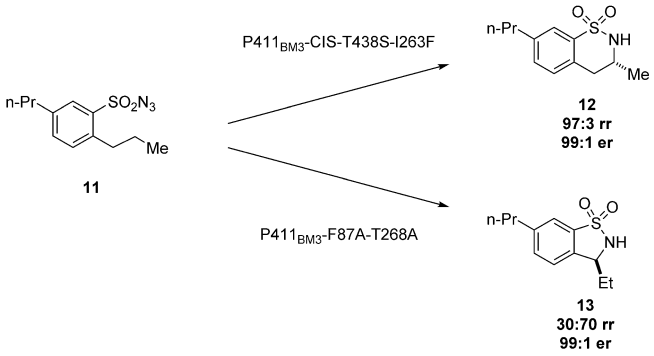

Figure 5. Regioselective nitrene insertion catalyzed by cytochrome $P411_{BM3}$. $P411_{BM3}$-CIS-T438S-I263F = V78A, F87V, P142S, T175I, A184V, S226R, H236Q, E252G, I263F, T268A, A290V, L353V, I366V, C400S, T438S, E442K.

Whereas the early reports of P450- and P411-catalyzed C–H amination used relatively rigid sulfonylazides as substrates, Fasan and co-workers found that more flexible carbonazidates can be converted into oxazolidinones in modest yield by using $P450_{BM3}$-FL#62.[26] A variety of carbonazidates were effective substrates, providing turnovers between 6 and 100, albeit with low enantioselectivity. The ease of synthesis opened the ability to explore the mechanism of enzyme-catalyzed amination reactions. Mechanistic studies using *cis*- and *trans*-homoallyl carbonazidates (**14** and **15**, respectively) show isomerization to the *trans*-oxazolidinone **16**, thereby suggesting that the reaction proceeds through C–H abstraction to generate a long-lived allylic or benzylic radical followed by radical recombination (Figure 6). Furthermore, kinetic isotope studies suggest C–H abstraction to be rate-limiting.

Serine-ligated $P411_{BM3}$ species are also capable of catalyzing intermolecular nitrene transfer reactions. Arnold and co-workers found that tosylazide (TsN_3, **18**) and sulfides provide sulfimides in modest yield under $P411_{BM3}$ catalysis (Figure 7).[27] The architecture of the active site is essential for catalysis in intermolecular nitrene transfer. In unoptimized active sites, the dominant product was reduction of the azide

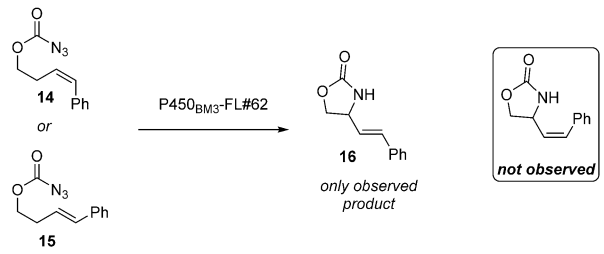

Figure 6. Mechanistic studies for the amination of C–H bonds catalyzed by $P450_{BM3}$-FL#62 suggest a long-lived allylic or benzylic radical.

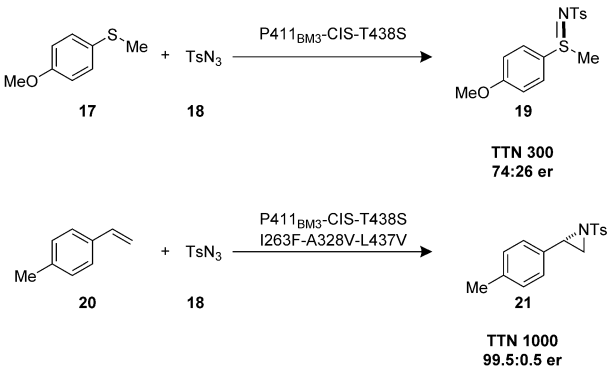

Figure 7. Sulfimidation and aziridination catalyzed by evolved cytochrome $P411_{BM3}$ variants.

to the corresponding sulfonamide. It is believed that this reduction occurs by electron transfer from the reductase domain of the P411 to the iron nitrenoid. In the presence of an optimized active site, sulfimidation becomes competitive with nitrenoid reduction. Hammett studies revealed a strong correlation between the electronic nature of the sulfide and the rate of sulfimidation, where electron-rich sulfides were amidated faster than electron-neutral sulfides.

Sulfimidation served as a gateway to the more challenging aziridination of alkenes (Figure 7).[28] Whereas protein scaffolds identified in the sulfimidation study provided only traces of aziridine, the introduction of I263F into the active site provided a substantial amount of aziridine, albeit with modest enantioselectivity. After two rounds of site-saturation mutagenesis to target residues in the active site, a variant was identified that provides aziridines in excellent enantioselectivity. In contrast to sulfimidation, where the electronic structure of the substrate largely dictates the substrate scope, the optimized aziridination catalyst tolerates an array of alkenes, where electronic structure has little effect on the reaction efficiency and selectivity.

2.2. Myoglobin-Catalyzed Reactions

Myoglobin is a heme protein that serves as an oxygen carrier in mammals but has no catalytic function. With respect to heme binding, myoglobin is structurally related to peroxygenases, where the iron center of the heme is ligated by

a histidine residue. Despite these similarities, myoglobin is less efficient than peroxidase in effecting oxidations.[29] This is attributed to the lack of a substrate binding cleft and the poorly positioned proximal histidine required to generate compound I. Hayashi and co-workers hypothesized that the absence of a binding cleft could be overcome by replacing the polar carboxylate groups of the heme with nonpolar aromatic groups.[30] By extracting the cofactor and reconstituting with a "double-winged cofactor", Hayashi and co-workers achieved superior reactivity for the oxidation of 2-methoxyphenol. This improvement was traced back to an increased affinity for the substrate (decrease in K_m). To increase the reactivity of the complex, Hayashi and co-workers explored mutation of the proximal histidine. By mutating histidine 64 to aspartic acid (H64D), the peroxidase activity was increased for myoglobin (Figure 8). Further replacement of the natural cofactor with the double-winged cofactor increased the peroxidase activity nearly 400-fold.

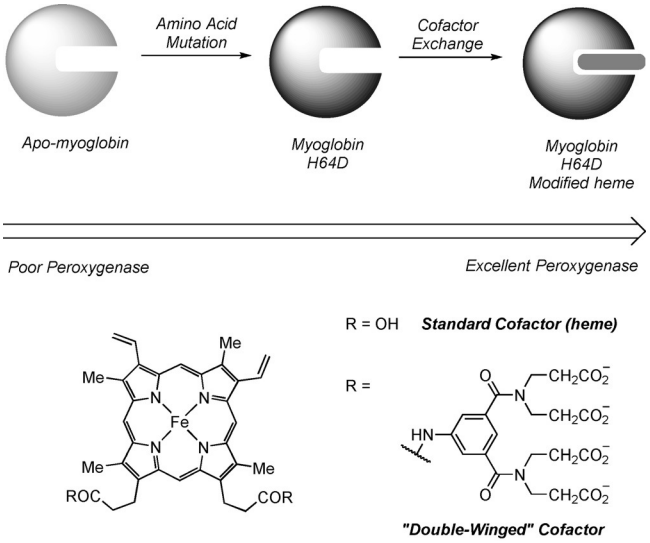

Figure 8. Repurposing myoglobin into a peroxygenase by chemogenetic optimization.

Imidazole-ligated iron porphyrins are known to be efficient small-molecule catalysts for carbene transfer reactions.[31] Sreenilayam and Fasan found that, in the presence of EDA and various primary and secondary anilines, myoglobin is able to effect carbene insertion into N–H bonds with efficiencies that surpass hemin alone (Figure 9).[32] As mentioned above, one drawback of wild-type myoglobin is its lack of a binding cleft. An active site can be carved out through mutation of the conserved distal histidine to valine (H64V) and mutation of a flanking valine to alanine (V68A). The improved catalyst provides excellent turnovers (TTN > 7500). In addition, it is also effective in coupling substituted styrenes with EDA to provide *trans*-cyclopropanes in high yield (TTN > 46000) and exquisite diastereoselectivity and enantioselectivity (Figure 9).[33] Mechanistic studies suggest that the cyclopropanation occurs via an electrophilic iron-carbenoid intermediate, which closely resembles the intermediate proposed for small-molecule catalysts.

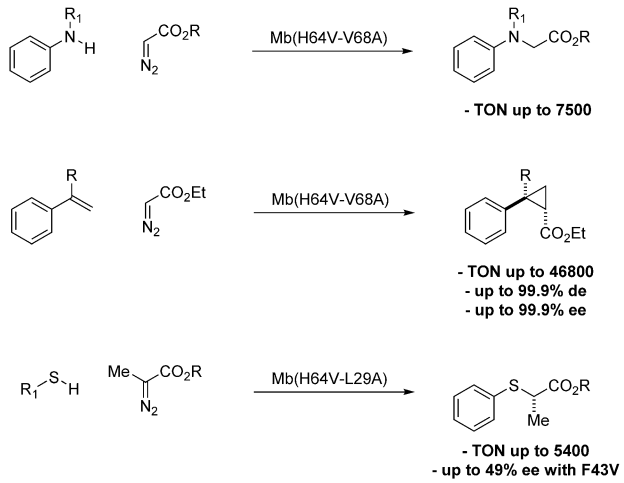

Figure 9. Myoglobin-catalyzed carbene insertion into N–H bonds, alkenes, and S–H bonds.

In addition to N–H insertion and cyclopropanation, myoglobin also catalyzes carbene insertion into S–H bonds.[34] In this case, however, the best variant for S–H insertion is L29A-H64V. This variant provides activity for a range of substituted aromatic and aliphatic thiols, a feat not possible with N–H insertion or cyclopropanation. Furthermore, sterically bulky cyclohexyl-, *tert*-butyl-, and benzyl-substituted diazoesters all provide excellent yields. A brief screen of active-site mutants provided a variant (F43V) that is capable of rendering this transformation asymmetric.

Similar to cytochrome P450s, myoglobin is also able to effect C–H amination by nitrene transfer, albeit in modest yield.[35] Mutation of the conserved distal histidine to valine (H64V) provides a modest increase in the catalyst activity. The enantioselectivity of the insertion can be modulated through modification of the active site. In general, myoglobin is less effective for reactions involving nitrenoid species than carbenoid species. To address this issue, Fasan and co-workers explored exchanging the heme cofactor by Mn and Co hemin species, which are known to be more effective for amination under organic conditions. Unfortunately, they were less effective that Fe hemin.

3. Supramolecular Docking

3.1. Biotin-Streptavidin-Based Artificial Metalloenzymes

Some of the best-studied artificial metalloenzymes take advantage of the strong noncovalent interactions between streptavidin (Sav) and biotinylated metal complexes.[36] The seminal report by Wilson and Whitesides demonstrated that [Rh(NBD)(**Biot-L**)]⊂avidin (Avi) (NBD = norbornadiene) could effect the hydrogenation of acetamidoacrylic acid (**22**) to (*R*)-acetamidoalanine (**24**) in modest enantioselectivity (up to 41 % *ee*).[9] (⊂ indicates supramolecular inclusion of the metal cofactor into the host protein.) Ward et al. re-examined this reaction by using streptavidin rather than avidin as the host protein. Streptavidin, similar to avidin, is a homotetra-

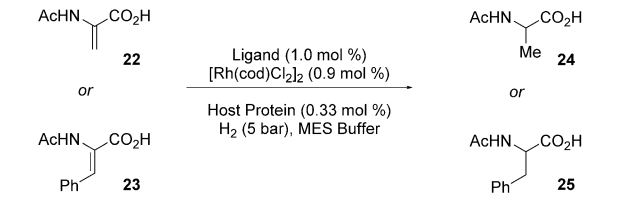

Entry	Ligand	Protein	% ee **24**	% conv **24**	% ee **25**	% conv **25**
1	**Biot-L**	WT Avi	37 (*S*)	90	-	-
2	**Biot-L**	WT Sav	92 (*R*)	Quant.	93 (*R*)	84
3	**Biot-L**	Sav S112G	96 (*R*)	Quant.	94 (*R*)	77
4	**Biot-4^{meta}-L**	Sav S112K	63 (*S*)	Quant.	88 (*S*)	89
5	**Biot-*(R)*-Pro-L**	Sav S112W	95 (*S*)	Quant.	95 (*S*)	Quant.

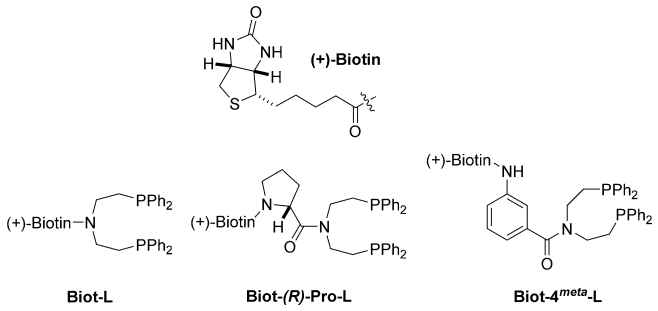

Figure 10. Artificial hydrogenase resulting from incorporation of a biotinylated Rh-diphosphine moiety within Sav variants. MES = 2-(*N*-morpholino)ethanesulfonic acid.

meric protein with a high affinity for biotin ($K_a > 10^{13}\,M^{-1}$).[37] It differs from avidin in its dielectric constant (p*l* = 6.2 for Sav versus p*l* = 10.4 for Avi) and ease of recombinant expression in *E. coli*. Upon switching from Avi to Sav, under otherwise similar reaction conditions, Ward and co-workers found that [Rh(cod)(**Biot-L**)]⊂WT Sav (cod = cycloocta-1,5-dienyl) furnished **24** in quantitative yield and 92 % *ee* (Figure 10).[38] The hybrid catalyst was also effective for the reduction of acetamidocinnamic acid (**23**) to (*R*)-acetamidophenylalanine (**25**) with 84 % conversion and 93 % *ee*.[39]

Ward and co-workers identified that modifying the amino acid spacer that links the metal to the biotin anchor can drastically vary the chemical environment in which the metal cofactor resides within streptavidin's "active site". More subtle fine-tuning can be achieved by genetic modification.[39,40] For example, site saturation at position S112 with [Rh(cod)(**Biot-L**)] provided two genetic mutants S112G and S112A which provided increased enantioselectivity for the *R* enantiomers of **23** and **24** (Figure 10). However, attempts to access the opposite enantiomer were unproductive by genetic modification alone. Testing 18 different chemical linkers provided two chemical linkers [Rh(cod)(**Biot-4^{meta}-L**)] and [Rh(cod)(**Biot-(*R*)-Pro-L**)] that yielded the *S* enantiomer preferentially.[41] Screening with Sav isoforms led to the identification of [Rh(cod)(**Biot-(*R*)-Pro-L**)]⊂S112W, which afforded both products in quantitative yield and 95 % *ee* (Figure 10).

A subsequent study by Reetz et al. explored a directed evolution strategy to optimize [Rh(cod)(**Biot-L**)]⊂Sav for the enantioselective reduction of methyl acetamidoacrylate.[42] Unfortunately, complications in protein expression required the use of small site-saturation mutagenesis libraries rather than large error-prone PCR libraries. Reetz et al. selected positions proximal to the active site (i.e. N49, L110, S112, L124). In the initial round, S112G was identified as a positive mutation that afforded product in 35 % *ee* in favor of the *R* enantiomer (compared to 23 % *ee* for WT Sav). A second round of mutagenesis furnished a double mutant N49V-S112G that provided the product in 54 % *ee*. When the N49V was evaluated alone it provided the best enantioselectivity in the study (65 % *ee*). After two rounds of mutagenesis, the opposite enantiomer (*S*)-acetamidoalanine methyl ester could be obtained in 7 % *ee* in the presence of [Rh(cod)-(**Biot-L**)]⊂Sav N49H-L124F.

Building on the hydrogenation of alkenes, Ward and co-workers explored biotinylated aminosulfonamide-ligated piano-stool complexes as catalysts for the transfer hydrogenation of ketones.[43] Mechanistically, transfer hydrogenation is distinct from classical hydrogenation in that the substrate does not coordinate to the metal center. Instead, the reaction is believed to proceed via a concerted transition state, whereby the hydride is delivered from the metal with a concomitant proton delivery from the amine ligand. A family of racemic-at-metal *N*-sulfonamide-1,2-ethylenediamine complexes where prepared from common Rh, Ir, and Ru piano-stool complexes and were screened against streptavidin isoforms. Biotinylation at the *para*-position of the sulfonamide universally provided more reactive complexes. Additionally, arene-capped ruthenium complexes provided the highest yields. The capping arene has a substantial impact on the enantiopreference of the reaction, with [(η^6-benzene)Ru(**Biot-*p*-L**)Cl] and [(η^6-*p*-cymene)Ru(**Biot-*p*-L**)Cl] favoring opposite enantiomers. This effect is most pronounced when combined with genetic mutations. For example, in the reduction of *p*-methylacetophenone, [(η^6-benzene)Ru(**Biot-*p*-L**)Cl]⊂WT Sav provides product with 89 % *ee* for the *R* enantiomer while [(η^6-*p*-cymene)Ru(**biot-*p*-L**)Cl]⊂WT-Sav provides the same product, but in only 29 % *ee* (*R*). When the same reactions are run with S112A, [(η^6-benzene)Ru(**biot-*p*-L**)Cl]⊂S112A provides product with 91 % *ee* in favor of the *R* enantiomer while [(η^6-*p*-cymene)Ru(**Biot-*p*-L**)Cl]⊂S112A provides the same enantiomer with 41 % *ee*. This enantiopreference can be inverted when lysine is used in place of alanine: [(η^6-benzene)Ru(**Biot-*p*-L**)Cl]⊂S112K provides product with 10 % *ee* in favor of the *S* enantiomer, while [(η^6-*p*-cymene)Ru(**Biot-*p*-L**)Cl]⊂S112A provides the *R* enantiomer with 63 % *ee*. It is thought that the presence of cationic residues in proximity to the metal center may change the interaction responsible for the enantioselectivity. When hydrophobic residues are close to the metal center, C–H···π interactions are may be responsible for selectivity. This interaction is likely overruled in favor of cation···π interactions when lysine is in proximity to the active site. A crystal structure of the streptavidin-bound metal complex revealed that residues K121 and L124 are in proximity to the metal center.

Initially, acetophenone derivatives were the only substrates to provide high enantioselectivity. Selectivity for

dialkyl ketone reduction was addressed using iterative rounds of site-saturation mutagenesis (Figure 11).[44] Building on the observation that the capping arene can favor different enantiopreference, Ward and co-workers conducted site-saturation mutagenesis on [(η^6-*p*-cymene)Ru(**Biot-*p*-L**)Cl] and [(η^6-benzene)Ru(**Biot-*p*-L**)Cl] with 4-phenyl-2-butanone. To accelerate the screening process, the streptavidin mutant was extracted from crude cell extracts using biotin-sepharose beads. Importantly, when Sav is present in excess, the sepharose-bound biotin only occupies one biotin-binding site, leaving the other three sites available for catalysis. It was quickly identified that the S112A and S112K variants favored the opposite enantiomers with both arene-capping groups, but with modest enantioselectivity. When these mutation were coupled with site-saturation libraries at positions K121 and L124, substantially improved enantioselectivities were achieved. For example, [(η^6-*p*-cymene)Ru(**Biot-*p*-L**)Cl]]⊂S112A-K121T provided 88% *ee* in favor of the *R* enantiomer, while [(η^6-*p*-cymene)Ru(**Biot-*p*-L**)Cl]⊂S112K-L124T favored the *S* enantiomer with modest enantioselectivity (26% *ee*). The enantioselectivity for the *S* enantiomer can be improved to 72% *ee* with [(η^6-benzene)Ru(**Biot-*p*-L**)Cl]⊂S112A-L121N. Interestingly, a single mutation to [(η^6-benzene)Ru(**Biot-*p*-L**)Cl]⊂S112A-L121W favors the *R* enantiomer with 84% *ee*. Collectively, this study suggests the importance of optimizing the genetic component of the artificial metalloenzymes for selectivity.

The reduction of alkenes and ketones using artificial metalloenzymes complements enzymes that are commonly used for industrial transformations (enoate reductases and ketoreductases).[45] Far less explored are the imine reductases, which have only recently been discovered.[46] In contrast, transfer hydrogenation has long been known to effect the enantioselective reduction of imines. The hydrogenation of cyclic imines could be effected in quantitative yield and modest enantioselectivity (57% *ee* (*R*)) by using [Cp*Ir(**Biot-*p*-L**)Cl]⊂WT Sav (Cp* = C_5Me_5).[47] Genetic optimization provides enhanced selectivity: [Cp*Ir(**Biot-*p*-L**)Cl]⊂S112A affords the *R* product with 91% *ee* and TTN > 4000 (Figure 12). A single point mutation with [Cp*Ir(**Biot-*p*-L**)Cl]⊂S112K affords the opposite enantiomer with 78% *ee* in favor of the *S* enantiomer.

The artificial imine reductase may be coupled to an amine oxidase (monoamine oxidase, MAO) to improve the enantiopurity of the amine.[48] In this cascade, the highly selective MAO selectively oxidizes the *S* amine back to the imine, to ultimately afford enantiopure *R* amine (Figure 13). This approach provides an elegant solution to the challenge of combining biocatalytic processes in tandem with small-molecule transition-metal catalysis. In general, it is understood that transition metals and enzymes suffer from mutual inhibition.[49] Compartmentalizing of the organometallic cofactor within a protein scaffold leads to deactivation being avoided. Furthermore, this allows the two reactions to be run in a single phase, rather than relying on a multiphase system.[50,51]

A challenge for artificial metalloenzymes is to overcome the loss of activity resulting from placing the metal in the active site of a protein. In the case of the imine reductase, the free metal cofactor is roughly 20 times more active than the artificial metalloenzyme in a WT-Sav (compare $k_{cat} = 21\ min^{-1}$; $K_m = 34$ mM to $k_{cat} = 1\ min^{-1}$; $K_m = 5$ mM for the free cofactor and [Cp*Ir(**Biot-*p*-L**)Cl]⊂WT-Sav).[52] Ward and co-workers hypothesized that charged residues within the active site might decrease the affinity of the greasy substrate for the active site. To address this challenge, hydrophobic residues were sequentially engineered into the active site to diminish the polarity of the pocket. The introduction of alanine residues at S112 and K121 (S112A-K121A) provided a substantial improvement in the catalytic efficiency, as reflected by an increase in k_{cat} ($24\ min^{-1}$) and decrease in K_m (15 mM; Figure 14). Collectively, these observations suggest that engineering the active site can increase the activity of the metal center without having affecting the direct metal coordination.

Metal coordination is another important feature when considering methods to generate active artificial metalloenzymes. When the metal is linked to biotin through the η^6-arene or η^5-cyclopentadiene ligand, rather than the aminosulfonamide ligand, a less-active metal complex for transfer hydrogenation of imines is formed. Ward and co-workers hypothesized that the coordination of histidine residues to the metal moiety could

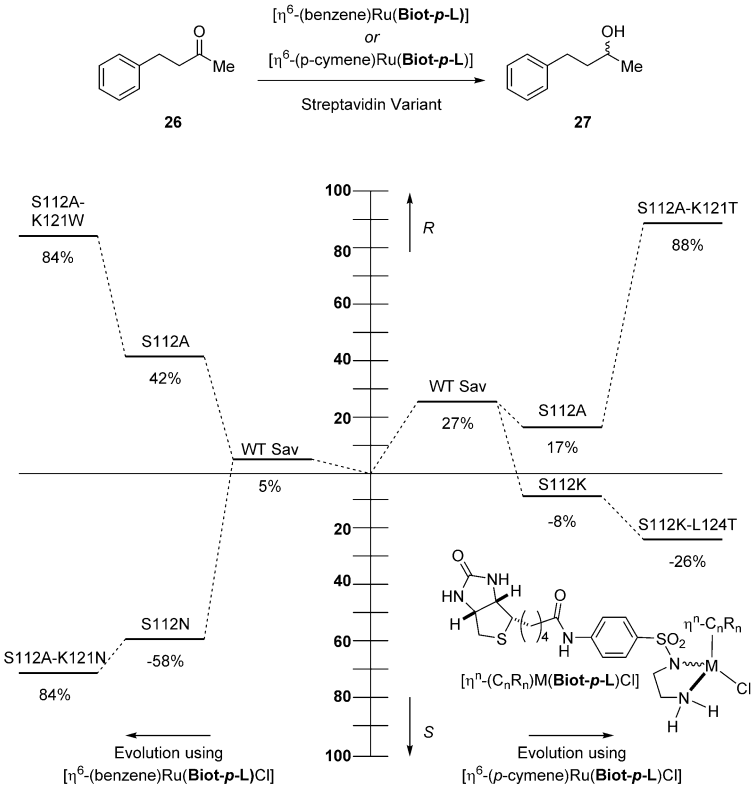

Figure 11. Evolutionary path for the most highly selective artificial transfer hydrogenase variants for the reduction of 4-phenyl-2-butanone (**26**).

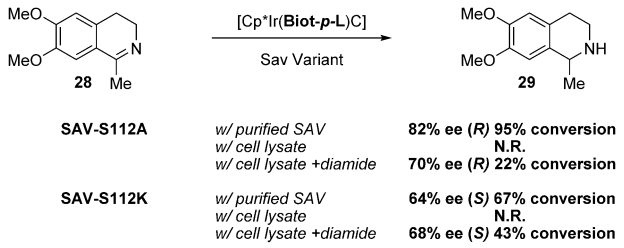

Figure 12. Reduction of dehydrosalsolidine (**28**) to salsolidine (**29**) using Sav-based artificial imine reductase either with purified samples or with cell lysates pretreated with diamide. N.R. = no reaction.

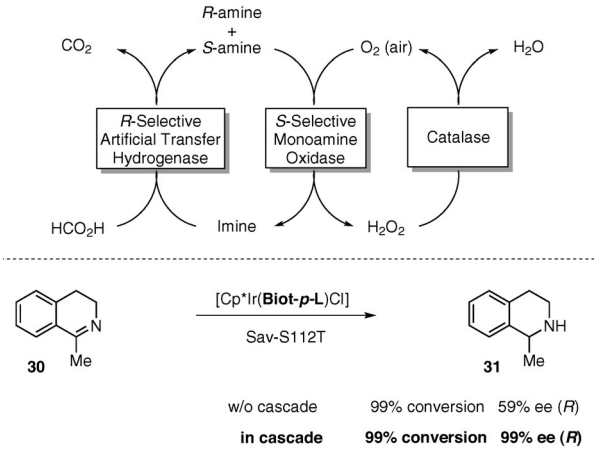

Figure 13. Artificial transfer hydrogenase in a cascade with a selective monoamine oxidase affords enantiopure cyclic *R* amines.

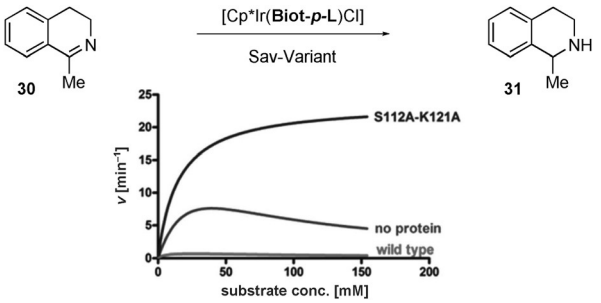

Figure 14. Genetic engineering of residues within the biotin-binding vestibule allows significant improvement of the catalytic efficiency of an artificial imine reductase based on the biotin–streptavidin technology. Reproduced with permission from the ACS.[52]

rescue the activity.[53] When histidine was introduced at S112 (i.e. S112H), the conversion of the reaction increases 10-fold over the wild-type complex to provide (*S*)-salsolidine (**29**) in quantitative yield and 55% *ee*. Interestingly, the enantioselectivity is inverted when histidine was introduced at position K121 (K121H), with (*R*)-salsolidine (**29**) generated in quantitative yield and 79% *ee* (Figure 15). Evaluation of the crystal structures of the two variants support the metal adopting very different orientations within the chiral biotin-binding vestibule depending on the position of the histidine residue, potentially accounting for the opposite enantioselectivities. Although, in general, metalloenzymes rely on genetic modification of the second coordination sphere, this study suggests that genetic optimization of the *first* coordination sphere can be used to enhance both the reactivity and the selectivity of artificial metalloenzymes.

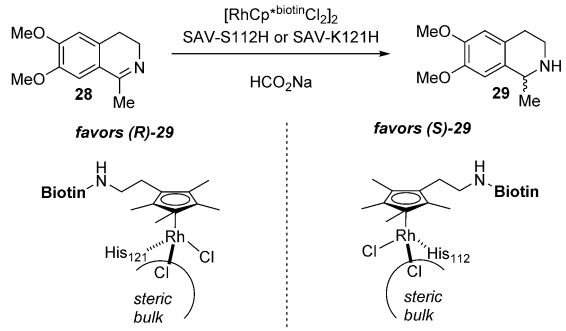

Figure 15. Activation of latent artificial metalloenzymes by coordination to a histidine residue affords artificial imine reductases. The position of the coordinating residue determines the enantiopreference of the reduction. $Cp^{*biotin} = Me_4C_5CH_2CH_2NHBiotin$.

The concept of protein coordination for increased reactivity was applied to the development of an artificial metalloenzyme for the Rh^{III}-catalyzed C–H activation of amides to provide dihydroisoquinolones (Figure 16).[54] With such catalytic systems, all three available coordination sites of the piano-stool complex are required for the reaction to proceed. Therefore, opportunities for an exogenous ligand to provide stereocontrol are limited. Ward, Rovis, and co-workers found that, in the presence of WT-Sav, a biotinylated {Cp*Rh} moiety provided enantioenriched product, but in low yield. Building on the fact that electrophilic C–H activation requires a base, often a carboxylate, to facilitate the C–H activation event, aspartate and glutamate residues were engineered in proximity to the metal. The productivity was enhanced when aspartic acid was introduced at K121D. The most active variant, N118K-K121E, provided a nearly 100-fold increase in activity compared to WT-Sav. When combined with the bulky tyrosine residue at position S112, a mutant (i.e. S112Y-K121E) was found that could provide

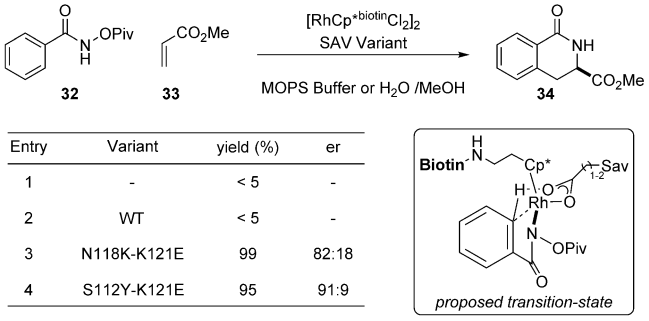

Figure 16. An artificial benzannulase results from incorporation of a biotinylated {Cp^*Rh^{III}} moiety within Sav. Engineering a basic residue at position 121 leads to a hundredfold increase in the rate. MOPS = 3-(*N*-morpholino)propanesulfonic acid.

high yield and enantioselectivity for the desired product. This represented the first example of an enantioselective Rh^{III}-C–H activation process and the first example of placing a mechanistically essential residue on the protein scaffold of an artificial metalloenzyme.

Artificial metalloenzymes are also able of catalyzing other reactions that were typically considered to be strictly limited to small-molecule catalysis. This is the case in the allylic alkylation of 1,3-diphenylallyl acetate (**35**; Figure 17).[55] It is

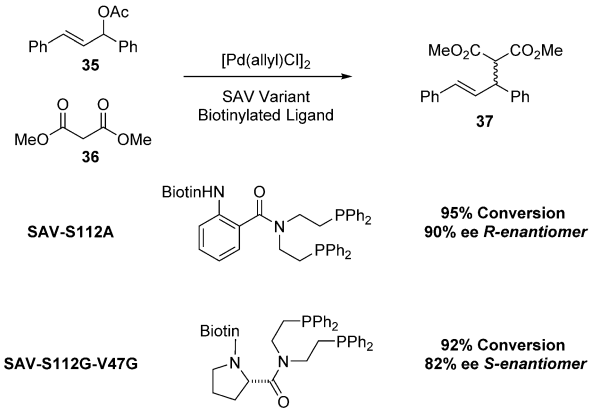

Figure 17. An artificial allylic allylase based on the biotin–streptavidin technology.

well known that soft nucleophiles directly attack the η^3-bound allyl moiety rather than proceeding through metal coordination followed by reductive elimination. Ward and co-workers found that the allylation occurs in high yield in modest selectivity when a biotinylated bis(phosphine) ligand is combined with a palladium catalyst. The mutant S112A provided the alkylated product **37** in excellent enantioselectivity. A single mutation S112Q afforded the opposite (*R*)-**37** with 31% *ee*. Introduction of an enantiopure (*R*)-proline spacer between the biotin anchor and the palladium complex, combined with the double mutant S112G-V47G, led to an increase in enantioselectivity in favor of the *R* enantiomer (up to 82% *ee* (*R*)).

Streptavidin-based artificial metalloenzymes can also be effective catalysts for enantioselective Suzuki reactions that form atropisomers (Figure 18). As a model reaction, 1-iodonaphthalene was coupled to 2-methoxy-1-naphthalene-

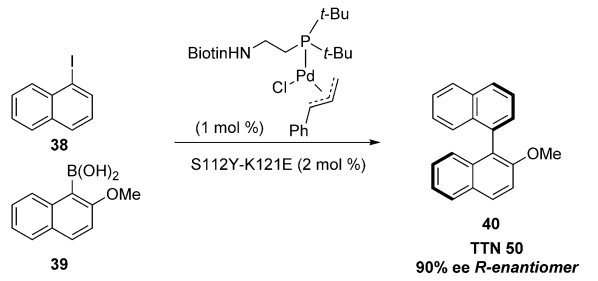

Figure 18. An artificial Suzukiase based on the biotin–streptavidin technology. Two point mutations improve the enantioselectivity from 58% to 90% *ee*.

boronic acid. After screening a small library of monodentate biotinylated ligands, it was found that electron-rich di-*tert*-butylphosphines provided the best yield. A screen of single mutants at position S112 and K121 revealed modest enantioselectivities for K121E (76% *ee* (*R*)). When this mutation was coupled with mutants at positions S112 or N118, a mutant capable of providing quantitative yield and 90% *ee* was achieved with S112Y-K121E. This hybrid catalyst is effective toward a variety of aryl iodides in excellent yield.[56]

3.2. Human Carbonic Anhydrase

Human carbonic anhydrase is responsible for the reversible conversion of CO_2 into bicarbonate.[57] Sulfonamides are known to inhibit this activity through coordination of their nitrogen atom to the catalytically active zinc center. Ward and co-workers prepared a family of aminopyridine and sulfonamide-pyridine ligands covalently linked to *p*-arylsulfonamides and tested their ability to effect the transfer hydrogenation of imines. The best results were observed with the sulfonamide-pyridine ligands, although mutagenesis of the flanking residues failed to provide increased yields or enantioselectivity (TTN 55, 32% *ee*; Figure 19). The X-ray

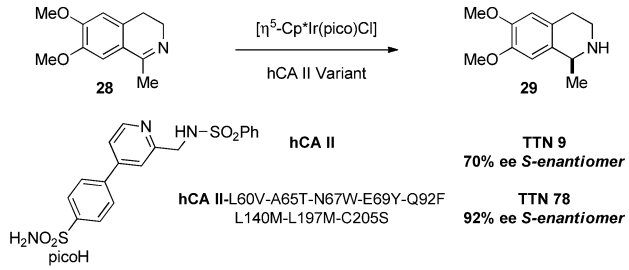

Figure 19. Artificial imine reductase based on the sulfonamide-carbonic anhydrase couple. In silico screening led to the identification of critical residues, ultimately allowing the affinity, the activity, and the enantioselectivity of the iridium-based hybrid to be significantly improved.

crystal structure of the artificial imine reductase revealed only a partial occupancy of the piano-stool moiety within the funnel-shaped hCAII binding site. The authors speculated that this may be caused by the shallow potential energy surface arising from the lack of stabilizing interactions between the piano-stool structure and the host protein. In collaboration with the Baker group, in silico screening led to the identification of up to eight mutations (L60V-A65T-N67W-E69Y-Q92F-L140M-L197M-C205S) that were predicted to improve the cofactor···hCAII interactions.[58] These mutants were expressed and tested for their affinity towards the sulfonamide-bearing cofactor. Gratifyingly, the affinity, the activity, and the selectivity were all significantly improved compared to the WT-hCA II, and provided product with 92% *ee* (Figure 19).

4. Covalent Anchoring

4.1. LmrR-Based Metalloenzymes

Roelfes and co-workers proposed that the hydrophobic pore of the transcriptional repressor from *L. lactis* (lactococcal multidrug resistance regulator, LmrR) might provide an effective environment for the generation of artificial metalloenzymes.[59] They thus selected LmrR, which in its dimeric form generates a flat hydrophobic pore to host artificial metal cofactors. By introduction of a cysteine residue into the hydrophobic active site, a Cu^{II}-phenanthroline moiety was bioconjugated into the hydrophobic pore. Initially, the complex was tested on the copper-catalyzed Diels–Alder reaction between ketone **41** and cyclopentadiene. Under optimized conditions, the metalloenzyme provided product in excellent conversion, high *endo* selectivity, and excellent enantioselectivity. Upon mutation of the flanking valine residue to alanine (V15A) the *endo/exo* selectivity increased with little loss of conversion or enantioselectivity (Figure 20). This scaffold was also applied to a copper-catalyzed oxa-Michael addition, but flanking mutations failed to provide any increase in the selectivity or yield.[60]

In these first-generation reports, Roelfes and co-workers took advantage of the bioconjugation of the ligand into the active site to localize the metal in the hydrophobic pore. The disadvantage of this approach is the addition of a step to prepare the catalyst. An alternative approach is to genetically engineer a non-natural amino acid with a side chain capable of ligating to the metal. By using AMBER codon suppression and a bipyridyl-alanine amino acid, Roelfes and co-workers generated an artificial metalloenzyme capable of catalyzing a vinylogous Friedel–Crafts reaction between a Michael acceptor and indole in modest yield.[61] Screening various mutations in the active site provided a variant, M89X-E107A, that provided product in 66% *ee*. The overall conversion could be increased to 58% by adding an additional mutation, M89X-N19A-E107A, but at the cost of enantioselectivity (14% *ee*).

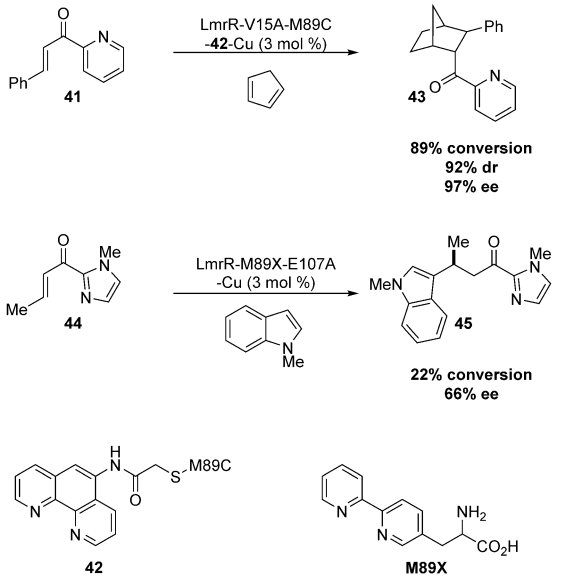

Figure 20. Relying on the LmrR as host protein, Roelfes and co-workers engineered either a phenanthroline, by bioconjucation, or a bipyridylalanine, using the AMBER codon suppression technology. The resulting artificial metalloenzyme catalyzes the Diels–Alder cycloaddition and the asymmetric Friedel–Crafts alkylation.

4.2. Prolyl Oligopeptidase

Typically, metal cofactors in artificial metalloenzymes reside near the surface of the protein of choice. While this can be effective for selective catalysis, a metal in a more enclosed active site could provide a more selective catalyst. Lewis and co-workers pioneered the covalent linking of metal cofactors to proteins by using strain-promoted azide–alkyne cycloadditions, where L-4-azidophenylalanine was genetically introduced through AMBER codon suppression (Figure 21 a).[62] Lewis and co-workers found that a Rh^{II} dimer can be introduced into the active site of prolyl oligopeptidase from *Pyrococcus furiosus* by mutation of the non-natural amino acid residue at position 477 (Z477), and expanding the active site by the introduction of alanine at four positions (E104, F146, K199, and D202).[63] The resulting protein, containing five mutations, was able to effect the cyclopropanation of styrene with donor–acceptor diazoesters in modest yield and enantioselectivity. When histidine was introduced in the active site at position 328 (H328), presumably to decrease conformational freedom and to block one rhodium center, the enantioselectivity increased to 47% *ee* and the product was formed in modest yield. The introduction of phenylalanine residues in the active site (F99–F594 or F99, F97) further optimizes the reaction to 74% yield and 92% *ee*. It is interesting to note that these mutations also substantially decrease the degree of diazo hydrolysis from 2:1 in favor of hydrolysis with the four alanine mutations, to about 5:1 in favor of cyclopropanation over hydrolysis with the best variant.

5. Artificial Hydrolases

Metallohydrolyases are ubiquitous in nature and serve various roles in cellular metabolism. There are numerous classes that rely on different metals to effect the desired transformations. Kim and co-workers set out to develop a new β-lactamase from a glyoxalase.[64] These enzymes differ both in the metal cofactor and in the nature of the active site. Kim and co-workers used a three-step approach to develop this new enzyme. The first was to remove the C-terminal domain required for substrate recognition in the glyoxylase II. Following this step, the enzyme's activity towards the natural substrate was completely suppressed. The second step was to introduce mutations to increase the affinity for zinc. This was achieved by introducing two cysteine residues as well as a tyrosine moiety and an aspartic acid to stabilize zinc binding. Finally, a new loop was introduced, based on sequence alignment with other metallo-β-lactamases. In the final step, a number of residues were randomized to allow for fine-tuning toward the selected β-lactam substrates. After

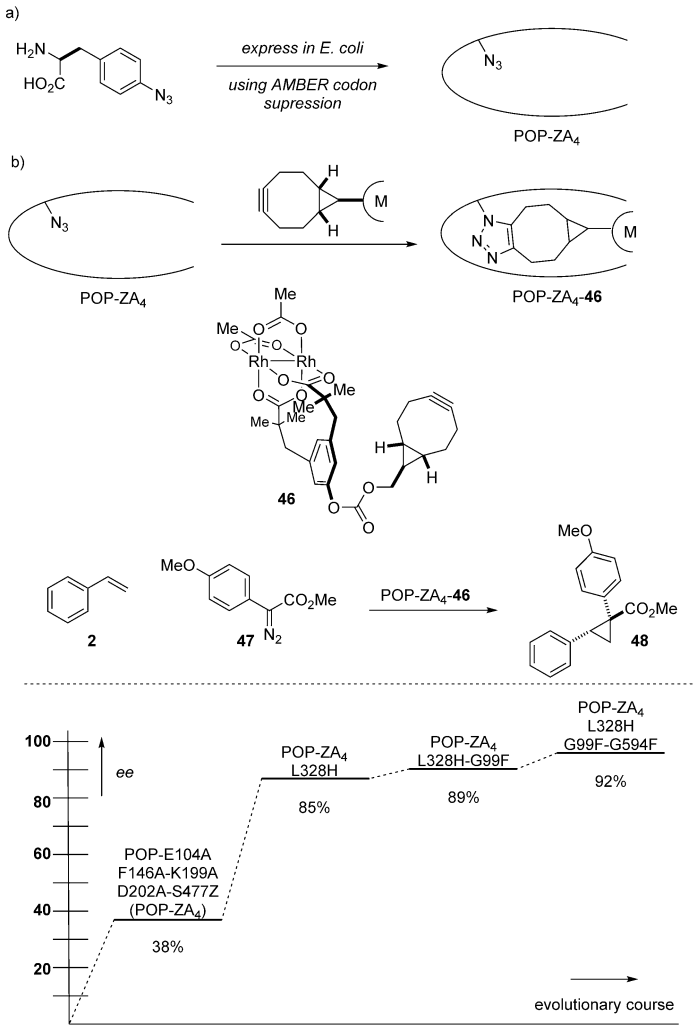

Figure 21. Evolutionary history for the genetically optimized artificial cyclopropanase using prolyl oligopeptidase from *Pyrococcus furiosus* (POP) as the host protein.

screening 2.1×10^7 mutants, 13 positive variants were identified. The best variant had most of the mutations in the substrate binding domain.

One could imagine generating a completely new protein fold to generate artificial metalloenzymes. This is particularly challenging in view of the difficulty in predicting tertiary and quaternary protein structures. Song and Tezcan have predicted, confirmed, and exploited the generation of quaternary structures by exploiting metal coordination (Figure 22).[65] In the course of these studies, metal binding was used to create and maintain the quaternary structure, while other metal centers served as catalysts. Appreciable activity was observed on *p*-nitrophenylacetate and ampicilline when a flanking lysine residues was mutated to alanine in the artificial folds generated from zinc and cb562 (a heme-containing four-helix bundle). The mutation of residues proximal to the catalytically active zinc-binding site provided a mutant with superior activity.

Metalloproteins that lack any catalytic function can be rendered catalytically active by directed evolution. Starting from a retinoid-X-receptor protein, Seelig and Szostak found that randomization of the two loops found in the zinc-finger domain of the protein can induce RNA-ligase activity.[66] To achieve this feat, an in vitro selection based on an mRNA display was employed. In these studies, the coding mRNA was covalently linked to its coded protein. Reverse transcription with a modified primer linked the substrate to the protein/mRNA catalyst. Treatment with a short RNA fragment and a biotinylated RNA fragment resulted in proteins that are capable of catalyzing the reaction that ligates the biotinylated fragment to the reverse transcription fragment. Selection and amplification allows the best catalyst to be identified. After 17 rounds of directed evolution, an RNA ligase was produced that provided a catalyst with multiple turnovers and a two-million-fold enhancement over the starting complex. This unique approach highlights the potential for achieving completely new reactivity.

Computational design has also been used to reappropriate enzyme function. Baker and co-workers used computation to repurpose the zinc-containing mouse adenosine deaminase into an organophosphate hydrolysase (Figure 23).[71] A search of the protein database (PDB) for proteins that contain zinc centers with one open coordination site coupled with rosetta design to reshape an active site to fit the geometry of the substrate provided 12 different designed proteins. Of the 12, 6 constructs were expressed as soluble proteins, but only one provided the desired reactivity. To further optimize the reactivity, 12 positions near the active site were mutated, including five that were identified by computational design. These 12 site-saturation libraries provided three improved mutants. Combining these mutations afforded a mutant with a 40-fold-increased activity over the parent construct. An additional round of error-prone polymerase chain reaction (PCR) led to the identification of three additional mutations. A final round of site-saturation mutagenesis provided a variant with an improvement of greater than 2500-fold over the parent protein. A comparison of the crystal structure with the computational model

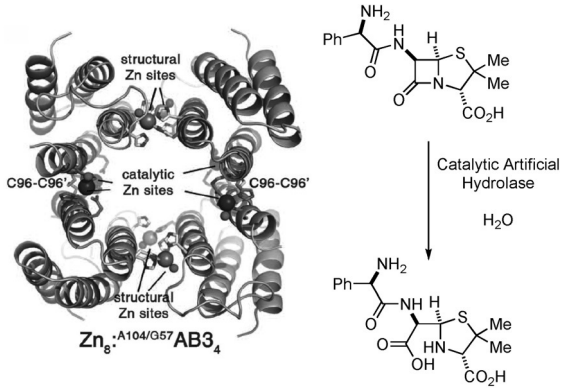

Figure 22. Artificial metallohydrolase resulting from supramolecular assembly (PDB 4U9D).

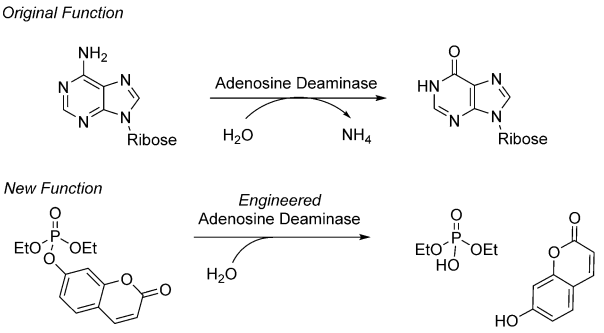

Figure 23. Artificial metallophosphatase resulting from computational design combined with directed evolution.

confirmed the exquisite predictive power (including side-chain orientation) of the rosetta design.

6. Outlook

Recent advances by the groups of Arnold and Fasan suggest a bright future for repurposing existing metalloprotein function to catalyze synthetically useful reactions that are new to nature. These heme-containing enzymes have evolved to function in a cellular environment; the repurposed enzymes can thus be screened either in vivo or in the presence of cell lysates. For directed-evolution purposes, this represents a major asset as this significantly speeds up the optimization process. The same holds true for the Zn-containing artificial hydrolases, which have been evolved without the need to rigorously purify the protein samples.[61–63]

In stark contrast, most abiotic metal-containing cofactors are inhibited in the presence of cellular extracts. This drawback also severely limits the use of transition-metal catalysts for chemical biology applications.[67] Interestingly, dirhodiumtetracarboxylate motifs have been shown to maintain their catalytic function in cell lysates.[68] This feature has been beautifully exploited by Lewis and co-workers to evolve an artificial cyclopropanase (Figure 21). This represents a rare example of a biocompatible precious-metal catalyst.[69] Alternatively, the chemical reagents (Michael acceptors or oxidants) have been exploited to neutralize inhibitors, thus enabling the screening of [Cp*Ir(**biot-*p*-L**)Cl] in the presence of cell lysates (Figure 12).[12] Affinity tags or chromatography may be exploited for the parallel purification of host proteins.[42,44]

In our view, the most exciting advances in artificial metalloenzymes may lie in the area of synthetic biology. Indeed, complementing metabolic pathways with the catalytic power of abiotic metal cofactors in vivo, may open fascinating perspectives for the synthesis of biofuels or high added-value products. To realize this however, several challenges remain: 1) cofactor uptake in vivo; 2) efficient cofactor bioconjugation, and 3) in vivo cascade reactions combining artificial metalloenzymes and natural enzymes.

Acknowledgements

T.R.W. thanks the Swiss National Science Foundation for generous continued support of research in the field of artificial metalloenzymes.

How to cite: *Angew. Chem. Int. Ed.* **2016**, *55*, 7344–7357
Angew. Chem. **2016**, *128*, 7468–7482

[1] a) U. T. Bornscheuer, G. W. Huisman, R. J. Kazlauskas, S. Lutz, J. C. Moore, K. Robins, *Nature* **2012**, *485*, 185; b) J. A. Gerlt, P. C. Babbitt, *Curr. Opin. Chem. Biol.* **2006**, *10*, 492.
[2] a) R. E. Cobb, N. Sun, H. Zhao, *Methods* **2013**, *60*, 81; b) P. A. Romero, F. H. Arnold, *Nat. Rev. Mol. Cell Biol.* **2009**, *10*, 866; c) C. Jäckel, P. Kast, D. Hilvert, *Annu. Rev. Biophys.* **2008**, *37*, 153; d) E. M. Brustad, F. H. Arnold, *Curr. Opin. Chem. Biol.* **2011**, *15*, 201.
[3] A. Currin, N. Swainston, P. J. Day, D. B. Kell, *Chem. Soc. Rev.* **2015**, *44*, 1172.
[4] a) H. E. Schoemaker, D. Mink, M. G. Wubbolts, *Science* **2003**, *299*, 1694; b) A. Zaks, *Curr. Opin. Chem. Biol.* **2001**, *5*, 130; c) A. Wells, H. P. Meyer, *ChemCatChem* **2014**, *6*, 918; d) N. J. Turner, A. Wells, *ChemCatChem* **2014**, *6*, 900; e) C. K. Savile et al., *Science* **2010**, *329*, 305; f) G. DeSantis et al., *J. Am. Chem. Soc.* **2003**, *125*, 11476.
[5] H. Renata, Z. J. Wang, F. H. Arnold, *Angew. Chem. Int. Ed.* **2015**, *54*, 3351; *Angew. Chem.* **2015**, *127*, 3408.
[6] a) E. Busto, V. Gotor-Fernańdez, V. Gotor, *Chem. Soc. Rev.* **2010**, *39*, 4504; b) B. K. Liu, X. F. Lin, *Curr. Org. Chem.* **2010**, *14*, 1966.
[7] S. K. Ma et al., *Green Chem.* **2010**, *12*, 81.
[8] a) K. Yamamura, E. T. Kaiser, *J. Chem. Soc. Chem. Commun.* **1976**, 830; b) H. L. Levine, Y. Nakagawa, E. T. Kaiser, *Biochem. Biophys. Res. Commun.* **1977**, *76*, 64.
[9] M. E. Wilson, G. M. Whitesides, *J. Am. Chem. Soc.* **1978**, *100*, 306.
[10] For recent reviews, see a) J. C. Lewis, *ACS Catal.* **2013**, *3*, 2954; b) M. Dürrenberger, T. R. Ward, *Curr. Opin. Chem. Biol.* **2014**, *19*, 99; c) T. Matsuo, S. Hirota, *Bioorg. Med. Chem.* **2014**, *22*, 5638; d) F. Yu, V. M. Cangelosi, M. L. Zastrow, M. Tegoni, J. S. Plegaria, A. G. Tebo, C. S. Mocny, L. Ruckthong, H. Qayyum, V. L. Pecoraro, *Chem. Rev.* **2014**, *114*, 3495; e) O. Pàmies, M. Diéguez, J.-E. Bäckvall, *Adv. Synth. Catal.* **2015**, *357*, 1567.
[11] A. Ilie, M. T. Reetz, *Isr. J. Chem.* **2015**, *55*, 51–60.
[12] Y. M. Wilson, M. Dürrenberger, E. Nogueira, T. R. Ward, *J. Am. Chem. Soc.* **2014**, *136*, 8928.
[13] a) G.-D. Roiban, M. T. Reetz, *Chem. Commun.* **2015**, *51*, 2208; b) J. A. McIntosh, C. C. Farwell, F. H. Arnold, *Curr. Opin. Chem. Biol.* **2014**, *19*, 126; c) R. Fasan, *Curr. Opin. Chem. Biol.* **2012**, *13*, 637.
[14] a) J. R. Wolf, C. G. Hamaker, J.-P. Djukic, T. Kodadek, L. K. Woo, *J. Am. Chem. Soc.* **1995**, *117*, 9194; b) B. Morandi, A. Dolva, E. M. Carreira, *Org. Lett.* **2012**, *14*, 2162.
[15] T. K. Hyster, F. H. Arnold, *Isr. J. Chem.* **2015**, *55*, 14.
[16] P. S. Coelho, E. M. Brustad, A. Kannan, F. H. Arnold, *Science* **2013**, *339*, 307.
[17] Z. J. Wang, N. E. Peck, H. Renata, F. Arnold, *Chem. Sci.* **2014**, *5*, 598.
[18] P. S. Coelho, Z. J. Wang, M. E. Ener, S. A. Baril, A. Kannan, F. H. Arnold, E. M. Brustad, *Nat. Chem. Biol.* **2013**, *9*, 485.
[19] T. Heel, J. A. McIntosh, S. C. Dodani, J. T. Meyerowitz, F. H. Arnold, *ChemBioChem* **2014**, *15*, 2556.
[20] Z. J. Wang, H. Renata, N. E. Peck, C. C. Farwell, P. S. Coelho, F. H. Arnold, *Angew. Chem. Int. Ed.* **2014**, *53*, 6810; *Angew. Chem.* **2014**, *126*, 6928.

[21] J. A. McIntosh, T. Heel, A. R. Buller, L. Chio, F. H. Arnold, *J. Am. Chem. Soc.* **2015**, *137*, 13861.
[22] H. Renata, Z. J. Wang, R. Z. Kitto, F. H. Arnold, *Catal. Sci. Technol.* **2014**, *4*, 3640.
[23] J. A. McIntosh, P. S. Coelho, C. C. Farwell, Z. J. Wang, J. C. Lewis, T. R. Brown, F. H. Arnold, *Angew. Chem. Int. Ed.* **2013**, *52*, 9309; *Angew. Chem.* **2013**, *125*, 9479.
[24] R. Singh, M. Bordeaux, R. Fasan, *ACS Catal.* **2014**, *4*, 546.
[25] T. K. Hyster, C. C. Farwell, A. R. Buller, J. A. McIntosh, F. H. Arnold, *J. Am. Chem. Soc.* **2014**, *136*, 15505.
[26] R. Singh, J. N. Kolev, P. A. Sutera, R. Fasan, *ACS Catal.* **2015**, *5*, 1685.
[27] C. C. Farwell, J. A. McIntosh, T. K. Hyster, Z. J. Wang, F. H. Arnold, *J. Am. Chem. Soc.* **2014**, *136*, 8766.
[28] C. C. Farwell, R. K. Zhang, J. A. McIntosh, T. K. Hyster, F. H. Arnold, *ACS Cent. Sci.* **2015**, *1*, 89.
[29] For efforts to convert myoglobin into an efficient peroxygenase, see S.-I. Ozaki, T. Matsui, Y. Watannabe, *J. Am. Chem. Soc.* **1996**, *118*, 9784.
[30] H. Sato, T. Hayashi, T. Ando, Y. Hisaeda, T. Ueno, Y. Watanabe, *J. Am. Chem. Soc.* **2004**, *126*, 436.
[31] T.-S. Lai, F.-Y. Chan, P.-K. So, D.-L. Ma, K.-Y. Wong, C.-M. Che, *Dalton Trans.* **2006**, 4845.
[32] G. Sreenilayam, R. Fasan, *Chem. Commun.* **2015**, *51*, 1532.
[33] M. Bordeaux, V. Tyagi, R. Fasan, *Angew. Chem. Int. Ed.* **2015**, *54*, 1744; *Angew. Chem.* **2015**, *127*, 1764.
[34] V. Tyagi, R. B. Bonn, R. Fasan, *Chem. Sci.* **2015**, *6*, 2488.
[35] M. Bordeaux, R. Singh, R. Fasan, *Bioorg. Med. Chem.* **2014**, *22*, 5697.
[36] For reviews, see a) T. R. Ward, *Acc. Chem. Res.* **2011**, *44*, 47; b) "Metal-Catalyzed Organic Transformations inside a Protein Scaffold Using Artificial Metalloenzymes": V. K. K. Praneeth, T. R. Ward, *Coordination Chemistry in Protein Cages*: *Principles*, *Design*, *and Applications* (Eds.: T. Ueno, Y. Watanabe), Wiley-VCH, Weinheim, **2013**, pp. 203 – 220.
[37] Y. Pazy, T. Kulik, E. A. Bayer, M. Wilchek, O. Livnah, *J. Biol. Chem.* **2002**, *277*, 30892.
[38] J. Collot, J. Gradinaru, N. Humbert, M. Skander, A. Zocchi, T. R. Ward, *J. Am. Chem. Soc.* **2003**, *125*, 9030.
[39] G. Klein, N. Humbert, J. Gradinaru, A. Ivanova, F. Gilardoni, U. E. Rusbandi, T. R. Ward, *Angew. Chem. Int. Ed.* **2005**, *44*, 7764; *Angew. Chem.* **2005**, *117*, 7942.
[40] M. Skander, N. Humbert, J. Collot, J. Gradinaru, G. Klein, A. Loosli, J. Sauser, A. Zocchi, F. Gilardoni, T. R. Ward, *J. Am. Chem. Soc.* **2004**, *126*, 14411.
[41] U. E. Rusbandi, C. Lo, M. Skander, A. Ivanova, M. Creus, N. Humbert, T. R. Ward, *Adv. Synth. Catal.* **2007**, *349*, 1923.
[42] M. T. Reetz, J. J.-P. Peyralans, A. Maichele, Y. Fu, M. Maywald, *Chem. Commun.* **2006**, 4318.
[43] a) C. Letondor, N. Humbert, T. R. Ward, *Proc. Natl. Acad. Sci. USA* **2005**, *102*, 4683; b) C. Letondor, A. Pordea, N. Humbert, A. Ivanova, S. Mazurek, M. Novic, T. R. Ward, *J. Am. Chem. Soc.* **2006**, *128*, 8320.
[44] M. Creus, A. Pordea, T. Rossel, A. Sardo, C. Letondor, A. Ivanova, I. LeTrong, R. E. Stenkamp, T. R. Ward, *Angew. Chem. Int. Ed.* **2008**, *47*, 1400; *Angew. Chem.* **2008**, *120*, 1422.
[45] a) J. Liang, J. Lalonde, B. Borup, V. Mitchell, E. Mundorff, N. Trinh, D. A. Kochrekar, R. N. Cherat, G. G. Pai, *Org. Process Res. Dev.* **2010**, *14*, 193; b) O. W. Gooding, R. Voldari, A. Bautista, T. Hopkins, G. Huisman, S. Jenne, S. Ma, E. C. Mundorff, M. M. Savile, *Org. Process Res. Dev.* **2010**, *14*, 119; c) J. Liang, E. Mundorff, R. Voldari, S. Jenne, L. Gibson, A. Conway, A. Krebber, J. Wong, G. Huisman, S. Trusdell, J. Lalonde, *Org. Process Res. Dev.* **2010**, *14*, 188; d) R. Stuermer, B. Hauer, M. Hall, K. Faber, *Curr. Opin. Chem. Biol.* **2007**, *11*, 203; e) C. M. Clouthier, J. N. Pelletier, *Chem. Soc. Rev.* **2012**, *41*, 1585.
[46] a) P. N. Scheller, S. Fademrecht, S. Hofelzer, J. Pleiss, F. Leipold, N. J. Turner, B. M. Nestl, B. Hauer, *ChemBioChem* **2014**, *15*, 2201; b) D. Wetzl, M. Berrera, N. Sandon, D. Fishlock, M. Ebeling, M. Müller, S. Hanton, B. Wirz, H. Iding, *ChemBioChem* **2015**, *16*, 1749.
[47] a) M. Dürrenberger, T. Heinisch, Y. M. Wilson, T. Rossel, E. Nogueira, L. Knörr, A. Mutschler, K. Kersten, M. J. Zimbron, J. Pierron, T. Schirmer, T. R. Ward, *Angew. Chem. Int. Ed.* **2011**, *50*, 3026; *Angew. Chem.* **2011**, *123*, 3082.
[48] V. Köhler, Y. M. Wilson, M. Dürrenberger, D. Ghislieri, E. Churakova, T. Quinto, L. Knörr, D. Häussinger, F. Hollmann, N. J. Turner, T. R. Ward, *Nat. Chem.* **2013**, *5*, 93.
[49] O. Pàmies, J.-E. Bächvall, *Chem. Rev.* **2003**, *103*, 3247.
[50] a) C. A. Denard, M. J. Bartlett, J. Wang, L. Lu, J. F. Hartwig, H. Zhao, *ACS Catal.* **2015**, *5*, 3817; b) C. A. Denard, H. Huang, M. J. Bartlett, L. Lu, Y. Tan, H. Zhao, J. F. Hartwig, *Angew. Chem. Int. Ed.* **2014**, *53*, 465; *Angew. Chem.* **2014**, *126*, 475.
[51] a) S. Wallace, E. P. Balskus, *Angew. Chem. Int. Ed.* **2015**, *54*, 7106; *Angew. Chem.* **2015**, *127*, 7212; b) G. Sirasani, L. Tong, E. P. Balskus, *Angew. Chem. Int. Ed.* **2014**, *53*, 7785; *Angew. Chem.* **2014**, *126*, 7919.
[52] F. Schwizer, V. Köhler, M. Dürrenberger, L. Knörr, T. R. Ward, *ACS Catal.* **2013**, *3*, 1752.
[53] J. M. Zimbron, T. Heinisch, M. Schmid, D. Hamels, E. S. Nogueira, T. Schirmer, T. R. Ward, *J. Am. Chem. Soc.* **2013**, *135*, 5384.
[54] T. K. Hyster, L. Knörr, T. R. Ward, T. Rovis, *Science* **2012**, *338*, 500.
[55] J. Pierron, C. Malan, M. Creus, J. Gradinaru, I. Hafner, A. Ivanova, A. Sardo, T. R. Ward, *Angew. Chem. Int. Ed.* **2008**, *47*, 701; *Angew. Chem.* **2008**, *120*, 713.
[56] A. Chatterjee, H. Mallin, J. Klehr, J. Vallapurackal, A. D. Finke, L. Vera, M. Marsh, T. R. Ward, *Chem. Sci.* **2016**, 6, 673.
[57] F. Monnard, E. Nogueira, T. Heinisch, T. Schirmer, T. R. Ward, *Chem. Sci.* **2013**, *4*, 3269.
[58] T. Heinisch, M. Pellizzoni, M. Dürrenberger, C. E. Tinberg, V. Köhler, J. Klehr, D. Häussinger, D. Baker, T. R. Ward, *J. Am. Chem. Soc.* **2015** 137, 10414.
[59] J. Bos, F. Fusetti, A. J. M. Driessen, G. Roelfes, *Angew. Chem. Int. Ed.* **2012**, *51*, 7472; *Angew. Chem.* **2012**, *124*, 7590.
[60] J. Bos, A. García-Herraiz, G. Roelfes, *Chem. Sci.* **2013**, *4*, 3578.
[61] I. Drienovská, A. Rioz-Martínez, A. Draksharapu, G. Roelfes, *Chem. Sci.* **2015**, *6*, 770.
[62] H. Yang, P. Srivastaca, C. Zhang, J. C. Lewis, *ChemBioChem* **2014**, *15*, 223.
[63] P. Srivastava, H. Yang, K. Ellis-Guardiola, J. C. Lewis, *Nat. Commun.* **2015**, *6*, 7789.
[64] H.-S. Park, S.-H. Nam, J. K. Lee, C. N. Yoon, B. Mannervik, S. J. Benkovic, H.-S. Kim, *Science* **2006**, *311*, 535.
[65] W. J. Song, F. A. Tezcan, *Science* **2014**, *346*, 1525.
[66] B. Seelig, J. W. Szostak, *Nature* **2007**, *448*, 828.
[67] E. M. Sletten, C. R. Bertozzi, *Angew. Chem. Int. Ed.* **2009**, *48*, 6974; *Angew. Chem.* **2009**, *121*, 7108.
[68] Z. T. Ball, *Acc. Chem. Res.* **2013**, *46*, 560.
[69] P. K. Sasmal, C. N. Streu, E. Meggers, *Chem. Commun.* **2013**, *49*, 1581.
[70] J. A. McIntosh, T. Heel, A. R. Buller, L. Chio, F. H. Arnold, *J. Am. Chem. Soc.* **2015**, *137*, 13861 – 13865.
[71] S. D. Khare, Y. Kipnis, P. J. Greisen, R. Takeuchi, Y. Ashani, M. Goldsmith, Y. Song, J. L. Gallaher, I. Silman, H. Leader, J. L. Sussman, B. L. Stoddard, D. S. Tawfik, D. Baker, *Nat. Chem. Biol.* **2012**, *8*, 29.

Received: September 20, 2015
Published online: March 11, 2016

